Investigation of the Modified Ballast Breakage Index for a Laboratory Test Series using the Proctor Compactor Machine

Erika Huschek-Juhász[1,2] and Szabolcs Fischer[1,2]

[1]Széchenyi István University, Central Campus Győr
Egyetem tér 1, H-9026 Győr, Hungary
{juhasz.erika,fischersz}@sze.hu

[2]Széchenyi István University, Vehicle Industry Research Center
Egyetem tér 1, H-9026 Győr, Hungary
[*]Corresponding author e-mail: fischersz@sze.hu

Abstract: The rock physics properties of the crushed railway ballast include resistance against breakage and wear. The qualification of such materials and their compliance with requirements is mainly considered by two standard tests: The Los Angeles abrasion and Micro-Deval wear resistance tests. These tests are indispensable for the legally mandatory qualification of aggregates, but several measurement methods have been developed that better simulate operating conditions and provide an even more accurate classification of these materials. A Proctor compactor machine was applied to induce a top impact load more similar to the operating conditions of ballast. Pre-screened, sorted, washed, and dried samples of andesite aggregate from four quarries with different rock physics characteristics were used to conduct the test series. The impact load was applied with increasing numbers of blows, i.e., 64, 128, 256 and 1024. Several parameters and indexes were calculated to reveal different relationships, which had to be modified in some cases to obtain estimates as close as possible to those obtained in individual tests. The original Ballast Breakage Index seemed to be an appropriate measure of the change in ballast material quality during deterioration for over a decade. The original calculation method was not consistent with the newly introduced test method. Keeping the principle, however, a modified BBI index calculation method has been developed that fundamentally simplifies the calculation of ballast fragmentation. The whole series of measurements aimed to provide, by material and number of impacts, a series of fragmentation and degradation curves for each of the three repeated measurements, which would give the degradation of samples with different rock physics and grain sizes.

Keywords: Ballast Breakage Index; BBI; Proctor compactor; Railway ballast; Rock physics; Fragmentation; Deterioration

1 Introduction

Railway vehicles (rolling stock) are in contact with the track via the rails, but the effects of this load are borne not only by the rails but also by the fastening system, the sleepers, the ballast, and the substructure [1]. Due to construction and maintenance deficiencies, as well as weather-related contamination, many track defects can significantly affect the lifetime of the entire railway track. These can appear as hidden and visible signs on the given track elements [2] [3]. Railway track operators worldwide pay particular attention to the deployment of various diagnostic systems and their regular measurement/operation to assess the need for maintenance work. Apart from the various specific track defects (corrugated wear, deflection of the rail end above at rail joints, water pockets, silting, and so on), the fragmentation and abrasion of the railway ballast are less noticeable. However, the deterioration of any element installed in a railway track can impact the track's (own) lifetime, given that in the event of a track failure, neighboring elements can also be damaged, and an accelerated self-excitation process can start. Due to its size, the railway ballast, which occupies the largest space at the cross-sectional level, deserves special attention, but its deterioration is not spectacular. In many countries, it is difficult to determine the exact timing of ballast bed cleaning (screening) or replacement.

In many cases, a trial screening is required. In some cases, deterioration models are given, but these are determined mainly based on the geometric deterioration of the track. Diagnostics executed by ground-penetrating radar (GPR) are also used. It is clear that the rock physics parameters of the ballast material, for example, and the particle size distribution (PSD) and content of fine ($d<0.5$ *mm*, where d is the diameter of grains) and finest ($d<0.063$ *mm*) at the time of installation, cannot be considered as a reliable predictor of the ballast particle breakage in the track, and therefore of the accurate time of necessary ballast cleaning and replacement. It should also be noted that rock physics parameters are not used to load and classify materials according to the stresses that will occur during actual or real operation in the railway permanent way. The railway operators and maintainers often apply the determination of the actual content of fine and finest in the ballast bed to compute the necessity of the above-mentioned work processes (i.e., screening or replacement); there are available experiences in these procedures [4]. The ballast itself is the primary source of the small particles in the ballast bed [5].

The current paper examines fragmentation, i.e., the breakage of a particle into several parts. Fine-grained material falling off the surface (abrasion) is present in all fines, but this effect is less pronounced.

2 Literature Review

2.1 Long-Term behavior of Railway Ballast

Railroads are important for sustainable transportation [6-9]. Public railways ensure energy-efficient transportation alternatives compared with roads [10] [11]. Utilizing railways can diminish urban congestion, lessen road (pavement) wear, and reduce emissions [12]. The railway permanent way consists of superstructure and substructure [13]; the ballast bed is part of the superstructure.

Railway ballast, a key component of track infrastructure, serves multiple functions: it distributes load, provides drainage, and maintains track stability. Over time, the efficacy of ballast in performing these functions is compromised due to particle breakage [14-16], a phenomenon resulting from the cyclic dynamic loading imparted by passing trains [17-20]. The long-term behavior of ballast is thus paramount, influencing decisions regarding maintenance, material selection, and track design.

Particle breakage occurs through various mechanisms, including crushing under direct load, attrition from particle-to-particle interactions, and environmental factors such as freeze-thaw cycles. Studies [21] [22] lay the groundwork for understanding how these processes reduce ballast effectiveness. The degradation of ballast particles not only impacts track geometry by causing settlement but also affects the drainage capabilities of the ballast layer, leading to water retention and further exacerbating degradation processes.

Studies conducted by Esmaeili et al. [23] and Guo et al. [24] contribute significantly to this understanding by comparing the performance of different ballast materials, such as steel slag versus limestone. These studies reveal that certain materials exhibit superior resistance to breakage, thereby offering the potential for longer service life and reduced maintenance needs.

The evaluation of ballast's long-term performance involves both empirical and computational approaches. Laboratory tests and field studies [25-28] provide direct observations of ballast behavior under real-world conditions, while computational models, including discrete element modeling [29-31] and finite element modeling [32], offer insights into the microscale interactions that contribute to particle breakage. The application of Digital Image Correlation (DIC) techniques [33] further enhances this analysis by allowing for the visualization of deformations and breakages within the ballast, providing a bridge between theoretical models and empirical evidence.

The intricate relationship between particle breakage and the long-term behavior of railway ballast underscores the complexity of maintaining track integrity. As particles degrade, the ballast layer becomes less capable of effectively distributing loads, increasing stress on track components and the subgrade. This can accelerate

track degradation, necessitating more frequent maintenance interventions and potentially leading to operational disruptions.

Furthermore, the accumulation of fines within the ballast layer, a direct consequence of particle breakage, impedes drainage, increasing the susceptibility of the track structure to water-related damage and further degrading the mechanical properties of the ballast.

Recognizing the challenges posed by particle breakage, recent advancements in ballast management have focused on innovative solutions to enhance ballast longevity and track performance. The exploration of alternative materials with improved durability [23] [24] and geosynthetic reinforcements [34] to distribute loads more evenly across the ballast bed represent significant strides toward mitigating particle breakage effects.

Additionally, deploying advanced diagnostic tools, such as GPR [35], facilitates early detection of problematic areas within the ballast layer, enabling targeted maintenance before minor issues escalate into significant failures. This proactive approach to maintenance, grounded in a detailed understanding of ballast's long-term behavior and the dynamics of particle breakage, holds promise for enhancing the resilience and sustainability of railway infrastructure.

2.2 Impact of Regulations on Aggregates; System of Materials to be Incorporated, Construction Product as a Concept

In Hungary and the international environment, the rules and regulations governing track rehabilitation (reconstruction, modernization) and new investments are becoming stricter. Without claiming to be exhaustive, there are also numerous regulations and directives governing the safety of work, the use of materials, the protection of our environment, and even the scope and existence of documents to be issued. The import and use of various products and the construction process are also subject to strict controls. In Hungary and the European Union, the aim is to ensure that certified products with a specific performance and application are placed on the market and installed in a project or upgrade.

The materials to be installed are primarily referred to as construction products [36].

Definition of "construction product" in Regulation (EU) No 305/2011:

" *any product or kit which is produced and placed on the market for incorporation in a permanent manner in construction works or parts thereof and the performance of which has an effect on the performance of the construction works with respect to the basic requirements for construction works".*

Regulation (EU) No 305/2011 (March 9, 2011) laying down harmonized conditions for the marketing of construction products and repealing Council Directive 89/106/EEC requires that the performance of specific categories of construction

products be certified by a declaration of performance [36]. The detailed rules for the design and installation of construction products in construction work and the certification of performance in this context are regulated and ordered under national competence by Government Decree 275/2013 (July 16, 2013) (hereinafter: the Decree) [36] [37].

The technical regulation sets out each construction product's specifications, product characteristics, and performance assessment methods. Technical specifications are drawn up by standardization bodies and, in the case of specific technical specifications, by technical assessment bodies. Technical specifications can be national standards, European harmonized standards, or, if the product is not covered by a national or European harmonized standard, a specific technical assessment for that product. This can be a National Technical Assessment ("NMÉ", i.e., "Nemzeti Műszaki Értékelés" *in Hungarian*) or a European Technical Assessment (ETA). The manufacturer decides which of the two documents is needed, as the NMÉ is only valid in Hungary, and the ETA allows the marketing of this product throughout the EU [36] [37].

Once the technical specification is in place, the next step is determined by the relevant technical specification (i.e., either the harmonized product standard or the NMÉ/ETA), but in all cases, the manufacturer must carry out a performance attestation procedure [36] [37].

Construction products are classified under “system codes”, based on their hazardousness.

The standard MSZ EN 13450:2003 [38] requires many tests to be carried out on rock masses (here, the railway ballast products), such as, but not limited to, the following rock classification tests:

- PSD
- (fine and) fines content
- grain (particle) size
- durability
- proportion of grains with crushed and broken surfaces
- resistance to fragmentation
- abrasion resistance
- surface wear resistance

The resistance to fragmentation and abrasion, as well as the classification into rock physics groups, is carried out using two standard tests, both past and present, the current abrasion resistance testing and determination of resistance to crushing tests:

- MSZ EN 1097-1:2024 Tests for mechanical and physical properties of aggregates. Part 1: Determination of the resistance to wear (micro-Deval)

[39] – i.e., the so-called micro-Deval wear test. The result is the *MDE* value in % unit.

- MSZ EN 1097-2:2020 Tests for mechanical and physical properties of aggregates. Part 2: Methods for the determination of resistance to fragmentation [40] – i.e., the so-called Los Angeles abrasion test. The result is the *LA* value in % unit.

The principle of the laboratory test methods also shows that the rock physics classification of crushed stones and particles is based on their strength and durability properties. Determining the strength properties of such aggregate building stone materials is carried out in the regulatory systems of the various countries either by the rotary drum or mortar test method. In Hungary, all the product standards are in force, and one or more rotating drum tests are used to assess the product's suitability [41].

3 Materials and Methods

3.1 Classical Test Method for Investigating Railway Ballast

The authors have executed many laboratory tests, of which the current paper deals exclusively with tests using the Proctor compactor machine. Any granular aggregate subjected to stresses above normal geotechnical ranges will exhibit significant particle fracturing. The degradation of ballast materials generally depends on several factors, including load amplitude, frequency, number of cycles, aggregate density, and grain angularity.

The standard Proctor mold and the Proctor compactor machine were used to design the latest study, where the Proctor compactor machine was not used the same way as the standard Proctor test (EN 13286-2:2010/AC:2012) [42]; only prewashed and dried particles were used in the testing mold and only for the calculable force. In a previous article [15], the specific energy [42] was calculated.

Samples of andesite rock material from four quarries, which can be used for railway construction, were processed and provided by Colas Északkő Ltd.: Tállya, Szob, Nógrádkövesd, and Recsk. 144 pieces of (4×3×3) samples were tested and divided into 1300 g (±5 g) portions.

For each quarry, the Los Angeles and Micro-Deval values per product were determined beforehand by an accredited metrology laboratory and are presented in Table 2. All the samples are the same as in the previous paper by the authors [15].

Several indices and parameters introduced by other researchers were calculated, the results of which were detailed in a previous article [15]:

- F_V [%] (here, the authors considered $F_V(AF)$)
- $d<22.4$ *mm*, $d<0.5$ *mm*, $d<0.063$ *mm* parameters and their changes
- d_{60}/d_{10} ratio (the abbreviation C_U is applied)
- *MA*, *MF*, and *Mavg* ("A" refers to the lower, "F" refers to the "upper", and "avg" relates to the "average")
- $\lambda(AF)$
- "AF" means after fatigue, and "BF" means before fatigue

Table 2
Los Angeles and Micro-Deval values according to standards [39, 40]

Products/quarries	**Tállya (T)**		**Szob (Sz)**	
	LA	***MDE***	***LA***	***MDE***
KZ 4/8	17.71	8.90	16.03	18.07
KZ 8/11	12.18	4.42	12.11	14.33
KZ 11/16	14.04	3.42	12.14	13.65
31.5/50	14.77	4.56	13.26	9.20
Products/quarries	**Nógrádkövesd (NK)**		**Recsk (R)**	
	LA	***MDE***	***LA***	***MDE***
KZ 4/8	19.78	22.10	22.20	13.92
KZ 8/11	16.58	18.30	17.46	10.42
NZ 11/22	20.95	20.43	19.22	9.17
31.5/50	10.02	10.30	18.02	11.53

Relatively significant changes were required in calculating the *BBI* values, as the grain sizes of the original single grain set required a value of zero for the smaller sets so that no meaningful number could be obtained for the pre-fatigue values. As a result, many *BBI* values (especially at low impact rates) were negative.

Rock physics suitability tests are of particular importance in domestic certification practice. Some experts believe that the Los Angeles test should retain its leading position in the future but that the test values can be compared with the test procedure developed for a broader overview. Therefore, these values have been pre-determined for each quarry by an accredited metrology laboratory (NZ, KZ, where NZ stands for fine crushed rock and KZ for special crushed rock), from which the single-grain test materials were separated and sieved to measure the correlations.

3.1 The Testing Procedure

The Proctor compactor machine, used for soil testing, was applied as the basic measuring instrument available for the provision, thus diversifying the research methods. The method developed here has been used in this form before, but the assembled sets were not loaded at this impact rate, and the material was not andesite,

so essentially, an additional measurement was developed [41]. Therefore, the basic idea for this type of study comes from foreign researchers.

The Proctor compactor machine was not applied in the same way as the standard Proctor test [42]; only prewashed and dried particles were used in the testing mold and only for the calculable force. The measurement design is shown in Fig. 1.

Figure 1
The measurement design [15]

The standard Proctor mold and the Proctor compactor machine's parameters are the following:

- mold diameter – "A" (d_1): 100 mm
- mold height – "A" (h_1): 120 mm
- height of fall (h_2): 457 mm
- diameter of base (d_2): 50 mm
- mass of rammer – "B" (m): 4.50 kg
- gravity acceleration (g): 9.81 m/s^2
- calculated impact surface: $0.25 \times d_1^2 \times \pi$=0.0314 m^2

The samples were sorted, and homogeneous sets of three different grain sizes were created for each material from each quarry: 6.3, 8.0 and 11.2 mm particles. So, the set of 3 grain diameters came from material from four different quarries. Each aggregate type was weighed three times (a new sample was loaded each time), so 144 samples were tested. The materials coming from the quarries were various commonly used mining products containing fractions of different sizes, so the original products were not used as mixed material on their own; occasionally, the mixing of single-grain samples from the same quarry was also broken. In all cases, the particles were used in washed and dried conditions.

Weighed samples of 1300 g were loaded into the standard working mold, filling the standard "cylinder". The impact of the hammer head on the test samples occasionally dispersed the particles from the pile, so a height adjuster of about 70 cm was used.

The number of blows was determined this way because, during the impacting labor, the size of the rammer head did not cover the entire diameter of the mold. The standard compactor machine rotates the cylinder continuously at given angles after each stroke. The full circle was made in 8 strokes (with a uniform load), so multiples of 8 were determined.

The number of blows is given as a quadratic increase.

After each load (64, 128, 256, and 1024 impacts/blows), the sample was disassembled as follows:

- After loading, the sample was compressed (i.e., the original starting height relative to the top of the mold was reduced) due to the fragmentation of the sample, so these subsidence values were measured.
- The loaded sample pieces were placed in a standard sieve, and after sieving, the following fractions were weighed separately: 11.2 mm, 8.0 mm, 6.3 mm, 4.0 mm, 2.0 mm, 1.0 mm, 0.5 mm, 0.25 mm, 0.125 mm, 0.063 mm, 0.0 mm.

After the measurement, the tested aggregate was thrown in the trash and not used again for another measurement.

At least three measurements were executed from each homogeneous sample, and the mean values of these measurements for a given sample were considered. After each measurement, a new set was created.

3.2 The Calculation Method

Particle size distribution curves also play a crucial role in determining rock physics properties, as these plots can clearly observe the degree of fracturing. This is how Indraratna and Lackenby developed and introduced a bedding material deterioration index (BBI) to quantify how the quality of bedding material changes during deterioration [44]. The initial and post-test particle size distribution curves are required to calculate the index. The calculation relationship is written in Eq (1) [44].

$$BBI = \frac{A}{A+B} \tag{1}$$

The *BBI* value is essentially an area calculation (or, in other words, an integral calculation) based on the resulting PSD curves. The area between the initial PSD and the final PSD after loading is the value of *A*. An arbitrary boundary of maximum breakage is defined. It is a linear line connecting the smallest sieve size of a given set (2.36 mm in [44]) to 95% of the largest grain size. The value B is the area

between the last-mentioned line and the final PSD. The *BBI* is essentially an area-based ratio based on the pre-degraded and post-degraded state.

The calculation of *BBI* was an adequate parameter in previous research [14] [15], and it was therefore necessary to adapt the method to the new measurement method.

Given that the tested aggregates were single-grain samples before the loading (fatigue), the initial PSD "curve" is a vertical line without exception. For a grain size of 11.2 mm, the vertical boundary is located in Fig. 2. With the appearance of the fragmented particles, the PSD of the fragmented, broken-off parts from the single-grain sample can be plotted. In the case of modification, the area between the initial PSD and final PSD is the *A* area (the unit is " mm×%"]; in this situation, it is between the vertical boundary line and under the curve of the given loading.

In the authors ' opinion, the area required to calculate the value of B causes difficulties because the arbitrary boundary of maximum breakage cannot be determined clearly. An option could be if the d_{95} and the 2.36 mm were adopted or synchronized from the railway ballast material [44]. However, the accurate line from the single-grain crushed material is not evident; there were a lot of assumed circumstances and hypothetical border conditions in the calculations. It is why a modified BBI value (the authors added its name BBI_{mod}) was also defined and obtained by area calculation, but only the fractional part, which is the modified calculation of *A*, was used. An illustration of the area calculation is shown in the Fig. 2.

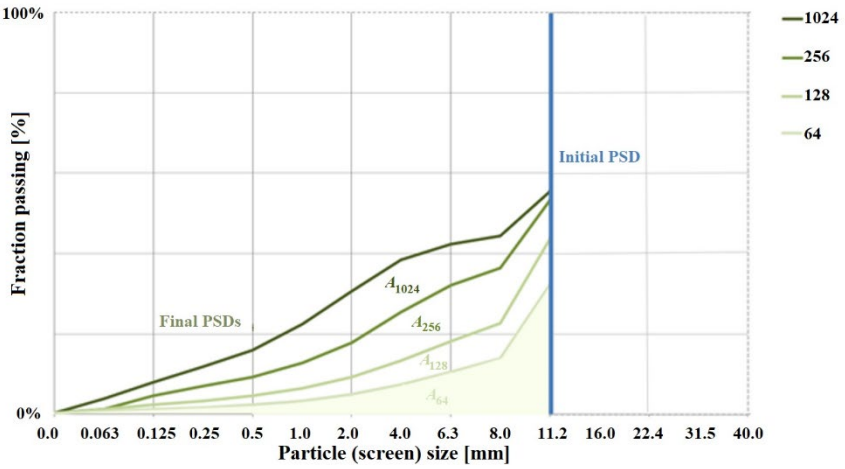

Figure 2

Calculation of BBI_{mod} based on the areas from A_{64} to A_{1024} (the considered lowest line is every time the horizontal axis at fraction passing of 0%)

4 Results and Discussion

4.1 BBI_{mod}

As expected from the design of the test method, every ballast set was highly fragmented after the impacts (blows), the aim being to determine the exact size of the set per quarry and fraction as a function of the number of blows, as was done in the previous article for several parameters [15].

Surprisingly, the homogeneous set of three sizes was so distinct regarding the results, as seen in Fig. 3 and Tables 3-5. Regarding BBI_{mod} values, the grain size of 6.3 mm illustrates the lowest values, i.e., the smallest area between the initial and final PSDs, while the 11.2 mm grain size clusters showed the highest values. Presumably, the grain size and the measurable accuracy of the fragmentation are related.

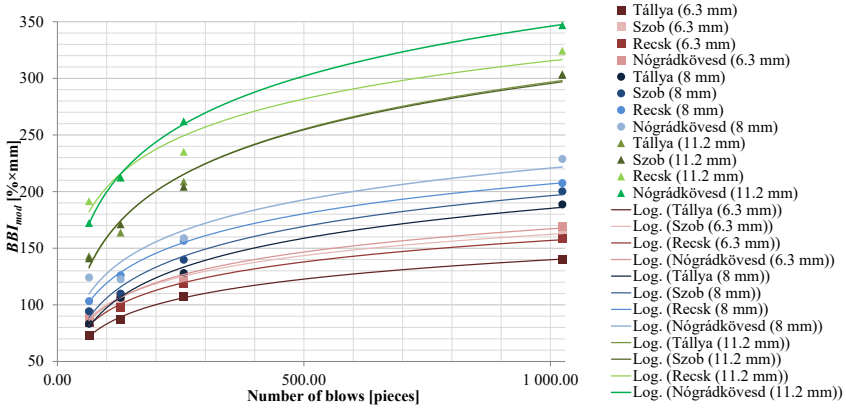

Figure 3
Presentation of calculated BBI_{mod} values

Table 3
Cumulative values based on 6.3 mm particle size following *LA* and *MDE* values [39,40]

6.3 mm						
Quarry/No. of blows (*x* [piece])		***BBI*$_{mod}$ [%×mm]**		***LA* [%]**	***MDE* [%]**	***LA*+*MDE* [%]**
Tállya (T)	**64**	73.0865	BBI_{mod}=59.7648·ln(*x*)– –116.1749 R^2=0.9811	17.71	8.90	26.61
	128	87.3082				
	256	107.1256				
	1024	140.4211				

Szob (Sz)	**64**	92.7902	BBI_{mod}=58.9811·ln(x)– –111.9715 R^2=0.9847	16.03	18.07	34.10
	128	101.8511				
	256	122.7082				
	1024	165.3998				
Recsk ®	**64**	84.3421	BBI_{mod}=48.4899·ln(x)– –19.5643 R^2=0,9649	22.20	13.92	36.12
	128	97.8419				
	256	118.4592				
	1024	158.7621				
Nógrádkövesd (Nk)	**64**	87.1749	BBI_{mod}=63.5061·ln(x)– –92.7180 R^2=0.9990	19.78	22.10	41.88
	128	107.3002				
	256	122.9519				
	1024	169.5485				

Table 4

Cumulative values based on 8.0 mm particle size following *LA* and *MDE* values [39, 40]

8 mm						
Quarry/No. of blows (*x* [piece])		***BBI*$_{mod}$ [%×mm]**		***LA* [%]**	***MDE* [%]**	***LA*+*MDE* [%]**
Tállya (T)	**64**	83.45031	BBI_{mod}=38.0975·ln(x)– –77.9892 R^2=0.9931	12.18	4.42	16.60
	128	106.2625				
	256	128.1730				
	1024	188.7797				
Szob (Sz)	**64**	94.3763	BBI_{mod}=39.23208·ln(x)– –74.6167 R^2=0.9870	12.11	14.33	26.44
	128	109.9813				
	256	139.9050				
	1024	200.2722				
Recsk ®	**64**	103.2940	BBI_{mod}=38.0365·ln(x)– –55.9495 R^2=0.9984	17.46	10.42	27.88
	128	126.1567				
	256	156.5324				
	1024	207.5296				
Nógrádkövesd (Nk)	**64**	124.1899	BBI_{mod}=40.4358·ln(x)– –58.5724 R^2=0.9280	16.58	18.30	34.88
	128	122.6374				
	256	158.9421				
	1024	228.8088				

Table 5
Cumulative values based on 11.2 mm particle size following *LA* and *MDE* values [39, 40]

11.2 mm						
Quarry/No. of blows (*x* [piece])		***BBI*$_{mod}$ [%×mm]**		***LA* [%]**	***MDE* [%]**	***LA*+*MDE* [%]**
Tállya (T)	**64**	143.1176	BBI_{mod}=24.6242·ln(x)– –30.2929 R^2=0.9980	14.04	3.42	17.46
	128	163.7892				
	256	208.7818				
	1024	303.8125				
Szob (Sz)	**64**	141.1132	BBI_{mod}=27.0494·ln(x)– –24.6189 R^2=0.9807	12.14	13.65	25.79
	128	171.0589				
	256	204.2317				
	1024	303.0696				
Recsk ®	**64**	191.5474	BBI_{mod}=27.3451·ln(x)– –32.0438 R^2=0.9944	19.22	9.17	28.39
	128	212.504				
	256	235.2345				
	1024	324.3869				
Nógrádkövesd (Nk)	**64**	172.3153	BBI_{mod}=29.5449·ln(x)– –36.9681 R^2=0.9944	20.95	20.43	41.38
	128	212.4072				
	256	262.1087				
	1024	346.8874				

The results from the PSD curves are illustrated in Table 6, considering the number of blows and the original (initial) grain sizes. The values represent the crushed parts' quantity, averages, standard deviations, and relative standard deviations. The lowest standard deviation and relative standard deviation for each aggregate type belonged to the 6.3 mm samples (indicated in the lightest blue). The lowest mean value was for the 8.0 mm aggregate, with higher mean values for larger grain sizes.

Table 6
Average (Avg.), standard deviation (SD), and relative standard deviation (RSD) of the crushed parts of the initial samples after the tests for different grain sizes (smallest values in light blue, largest values in dark blue)

***x* [piece]**	**Grain size [mm]**	**Avg. [%]**	**SD [%]**	**RSD [%]**
64	6.3	27.77	6.80	24.49
	8.0	23.03	14.08	61.15
	11.2	30.06	12.27	40.81

128	6.3	34.94	5.73	16.40
	8.0	29.47	7.72	26.19
	11.2	36.72	11.91	32.43
256	6.3	43.00	5.03	11.70
	8.0	39.61	8.45	21.32
	11.2	42.43	11.13	26.23
1024	6.3	58.10	4.14	7.12
	8.0	56.91	5.85	10.28
	11.2	60.59	7.44	12.27

The experience described in the paragraph above confirms that the loading of the smaller grain size shows a more minor variance in the measurement results. Interestingly, the pattern of coloring was exactly the same for 128 and 1024 blows.

Based on the values presented in Fig. 3 and Tables 3-6, the following conclusions can be drawn:

- Presumably, the grain size and the scatter of the measurement results are related.
- The highest BBI_{mod} values were obtained for loading the 11.2 mm single-grain samples, while the smallest values were obtained for the 6.3 mm. The measured *LA* and *MDE* values essentially confirm a tendency for fragmentation.
- For BBI_{mod}, a clear and strong correlation (considering logarithmic regression functions) was observed with the value of the number of impacts.
- In all cases, BBI_{mod} values follow a logarithmic trend with increasing load.

Similar regression functions describe the deterioration processes for the crushed stones (KZ and NZ) from the quarries Tállya, Szob, and Recsk. The notable exception in all cases was the Nógrádkövesd crushed stones for all fractions, presumably due to their poorer, weaker rock physics, i.e., the highest fragmentation and abrasion properties (see *LA* and *MDE* values in Table 2).

The developed method had been used in this form before, but the samples were not loaded with this impact number, and the material was not andesite, so essentially, an additional measurement was developed [43].

It is necessary to note that the samples tested were, on the one hand, small in size. This means that instead of the 31.5/50 mm or 31.5/63 mm products typical of railway crushed stone bedding, single grain samples (aggregates) of 4/8 mm, 8/11 mm, 11/16 mm, and 11/22 mm crushed stone products were tested under laboratory conditions: grain sizes of 6.3 mm, 8.0 mm, and 11.2 mm. The samples for testing were selected from the same blasted rock stockpile from each andesite quarry.

The BBI_{mod} value can be used for comparison and regression analysis, but a more detailed analysis was needed to see exactly how the aging trends depend on the *LA*, *MDE,* and possibly *LA+MDE* parameters/values.

4.2 Investigation of Deterioration Trends

According to the F_V parameter, the intervention threshold is generally 80% (varies by country) [44].

According to the (original) *BBI* parameter, the intervention threshold is 1.0 [44].

The standard MSZ EN 13450:2003 [38] considers the 22.4 mm sieved fraction to be essentially the smallest, with a value accepted for production not exceeding 3 (or a maximum of 7) % by weight for new (fresh) ballast. Based on domestic practice, a ballast cleaning machine removes particles (so-called grit) of d<20...23 mm from the ballast bed so that the need to remove a fraction of less than 22.4 mm by weight of the total sample weight exceeding 30% can be taken as a basis for determining the theoretical ballast grade(s) (i.e., *d<22.4 mm* > 30%) during maintenance [14, 45]. Along this logic, it was examined where, within the homogeneous aggregates (6.3, 8.0, and 11.2 mm), the 22.4 mm sieve value of the standard sample is found in proportion. Proportioning yielded the values shown in Table 7.

Table 7

Sieve sizes defined for the sizes of the aggregates, at which smaller fractions are already treated as fine grains

Aggregate grain size	**31.5/50**	**11.2 mm**	**8.0 mm**	**6.3 mm**
***d* sieve size determined based on grain size (fine fraction limit)**	22.4 mm	6.3 mm	4.0 mm	~4.0 mm

Table 8 shows how the number of blows for different fractions was determined by interpolation for the 30% fine fraction limit [45].

Table 8

Determination of the rusting cycle time based on the results of the Proctor test

Quarry		**Real operating conditions 31.5/50 mm**		**Proctor-test 11.2 mm**		**Proctor-test 8.0 mm**		**Proctor-test 6.3 mm**	
	Fine fraction limit	*d<22.4 mm*		*d<6.3 mm*		*d<4.0 mm*		*d<4.0 mm*	
Tállya (T)	**Calculating the number of**	13 years 8,666,671 axles	**30%**	256	18.84%	256	15.72%	256	17.39%
				ca. 540	**30%**	**ca. 700**	**30%**	**ca. 800**	**30%**
				1024	44.69%	1024	37.33%	1024	32.40%

	axles passed			*1 blow = 16,049 theoretical axles*		*1 blow = 12,380 theoretical axles*		*1 blow = 10,833 theoretical axles*	
				$axles_{avg}$×blows = 13,000×1024			***13,312,000 axles (20 years)***		
Nógrád-kövesd (Nk)				128	18.18%	256	23.01%	256	26.30%
				ca. 240	**30%**	**ca. 400**	**30%**	**ca. 450**	**30%**
				256	32.18%	1024	49.99%	1024	48.72%
				1 blow = 36,111 theoretical axles		*1 blow = 21,667 theoretical axles*		*1 blow = 19,259 theoretical axles*	
				$axles_{avg}$×blows = 25,680×1024			***26,295,322 axles (40 years)***		
Szob (Sz)				256	18,43%	256	15,62%	256	19,94%
				ca. 580	**30%**	**ca. 680**	**30%**	**ca. 580**	**30%**
				1024	42.30%	1024	38.90%	1024	40.95%
				1 blow = 14,943 theoretical axles		*1 blow = 12,745 theoretical axles*		*1 blow = 14,943 theoretical axles*	
				$axles_{avg}$×blows = 14,210×1024			***14,551,100 axles (21.8 years)***		
Recsk ®				256	17.64%	256	19.27%	256	21.21%
				ca. 530	**30%**	**ca. 580**	**30%**	**ca. 590**	**30%**
				1024	43.22%	1024	42.70%	1024	41.49%
				1 blow = 16,352 theoretical axles		*1 blow = 14,943 theoretical axles*		*1 blow = 14,689 theoretical axles*	
				$axles_{avg}$×blows = 15,328×1024			***15,695,787 axles (23.5 years)***		

In real conditions, the ballast must be cleaned (re-screened) after installation if the percentage by weight of material passing through the 22.4 mm sieve (as a proportion of the total pile) exceeds 30%, i.e., if the material is so contaminated ($d<22.4$ *mm* > 30%) [4]. In Table 8, the authors assumed that the appearance of the proportionally similar smallest fraction ($d<4$ *mm*, $d<6.3$ *mm*) occurred much sooner in the Proctor compactor measurement, as measured by impact counts. The 30% fragmentation is reached at an average of 555 blows (473 blows for 11.2 mm, 590 for 8 mm, and 605 for 6.3 mm), representing a very high level of destruction.

On this basis, a nominal/defined degree of fragmentation can be achieved in a relatively short time by the test method, which is consistent with the parameters in use. For the 30% values for $d<4$ *mm* and $d<6.3$ *mm* (only), theoretical shaft displacements have been calculated so that a theoretical cycle time, failure duration (calculated, predictable years) can be assumed. The Nógrádkövesd material showed exceptionally high values, on average twice as high as the andesite material from the other three mines, which show results in the same range of values. If the results of the Nógrádkövesd material are not included in the average calculation, the average number of impacts for a 30% failure rate is 653 (550 blows for 11.2 mm, 653 blows for 8 mm, 656 blows for 6.3 mm).

Conclusions

This study investigated the durability and fragmentation of railway ballast using a modified Ballast Breakage Index (BBI_{mod}), applying a Proctor compactor machine for more accurate simulation of real-world conditions. The authors utilized andesite aggregates from four quarries, subjecting them to varied impact loads to analyze breakage and wear resistance. They introduced and developed a new index (BBI_{mod}) and its simplified calculation method to accurately evaluate ballast fragmentation, addressing limitations of the original *BBI* under new test conditions. The paper demonstrated a clear logarithmic correlation between the number of impacts and fragmentation degree, highlighting the impact of rock physics characteristics and grain sizes on ballast durability. BBI_{mod} values show a strong, consistent relationship with applied load, aiding in accurately assessing ballast material quality.

Moreover, the study enhanced the selection process for railway ballast materials, potentially extending track lifetimes and reducing maintenance requirements. It highlighted the importance of refining testing methods to reflect operational conditions more closely, paving the way for further optimization in ballast material use. As a main conclusion, the paper advanced the methodology for evaluating railway ballast deterioration, offering a more operationally relevant and reliable approach to assessing ballast quality through the modified Ballast Breakage Index (BBI_{mod}).

Acknowledgement

The research was supported by SIU Foundation's project 'Sustainable railways – Investigation of the energy efficiency of electric rail vehicles and their infrastructure'. The publishing of the paper received neither financial support, nor financing for the article process charges.

References

[1] P. Vaszary, F. Kiss. Railway maintenance. Tankönyvkiadó, Budapest, 1990 (in Hungarian)

[2] J. Pintér. Maintenance of the railway superstructure. MÁV. Budapest, 1991 (in Hungarian)

[3] G. Kormos. Railway construction and maintenance, BME, Budapest, 2010 (in Hungarian)

[4] Plasser. Internal research report of the company Plasser S1, Tamping unit penetration tests of an 09-16 and an 07-32 tamping machine in ballast bed, 1998 (in German)

[5] E. T. Selig, J. M. Waters. Track Geotechnology and Substructure Management, Thomas Telford Services Ltd., London, UK, London, 1994, https://doi.org/10.1680/tgasm.20139

[6] M. Kurhan, D. Kurhan, N. Hmelevska. Innovative Approaches to Railway Track Alignment Optimization, in Curved Sections. Acta Polytechnica Hungarica, Vol. 21(1), 2024, pp. 207-220, https://doi.org/10.12700/APH.21.1.2024.1.13

[7] D. M. Kurhan. Entropy Application for Simulation the Ballast State as a Railway Element. Acta Polytechnica Hungarica, Vol. 20(1), 2023, pp. 63-77, https://doi.org/10.12700/APH.20.1.2023.20.5

[8] O. Nabochenko, M. Sysyn, U. Gerber. Krumnow, N. Analysis of Track Bending Stiffness and Loading Distribution Effect in Rail Support by Application of Bending Reinforcement Methods. Urban Rail Transit, Vol. 9(2), 2023, pp. 73-91, https://doi.org/10.1007/s40864-023-00194-1

[9] V. Atapin, A. Bondarenko, M. Sysyn, D. Grün. Monitoring and evaluation of the lateral stability of CWR track. Journal of Failure Analysis and Prevention, Vol. 22(1), 2022, pp. 319-332, https://doi.org/10.1007/s11668-021-01307-3

[10] B. Ramazan, R. Mussaliyeva, Z. Bitileuova, V. Naumov, I. Taran. Choosing the logistics chain structure for deliveries of bulk loads: Case study of the Republic Kazakhstan. Naukovyi Visnyk Natsionalnoho Hirnychoho Universytetu, Vol. 2021(3), 2021, pp. 142-147, https://doi.org/10.33271/nvngu/2021-3/142

[11] G. Nugymanova, M. Nurgaliyeva, Z. Zhanbirov, V. Naumov, I. Taran. Choosing a servicing company's strategy while interacting with freight owners at the road transport market. Naukovyi Visnyk Natsionalnoho Hirnychoho Universytetu, Vol. 2021(1), 2021, pp. 204-210, https://doi.org/10.33271/nvngu/2021-1/204

[12] S. Fischer, S. Kocsis Szürke. Detection process of energy loss in electric railway vehicles. Facta Universitatis, Series: Mechanical Engineering, Vol. 21(1), 2023, pp. 81-99, https://doi.org/10.22190/FUME221104046F

[13] S. Fischer. Evaluation of inner shear resistance of layers from mineral granular materials. Facta Universitatis, Series: Mechanical Engineering, 2023, https://doi.org/10.22190/FUME230914041F

[14] S. Fischer. Breakage test of railway ballast materials with new laboratory method. Periodica Polytechnica Civil Engineering, Vol. 61(4), 2017, pp. 794-802, https://doi.org/10.3311/PPci.8549

[15] E. Huschek-Juhász, A. Németh, M. Sysyn, G. Baranyai, J. Liu, S. Fischer. Testing the fragmentation of railway ballast material by laboratory methods using Proctor compactor. Naukovyi Visnyk Natsionalnoho Hirnychoho Universytetu, Vol. 2024(1), 2024, pp. 58-68, https://doi.org/10.33271/nvngu/2024-1/058

[16] L. Ézsiás, R. Tompa, S. Fischer. Investigation of the Possible Correlations Between Specific Characteristics of Crushed Stone Aggregates. Spectrum of Mechanical Engineering and Operational Research, Vol. 1(1), 2024, pp. 10-26, https://doi.org/10.31181/smeor1120242

[17] A. Németh, S. Fischer. Investigation of the glued insulated rail joints applied to CWR tracks. Facta Universitatis, Series: Mechanical Engineering, Vol. 19(4), 2021, pp. 681-704, https://doi.org/10.22190/FUME210331040N

[18] A. Brautigam, S. Szalai, S. Fischer. Investigation of the application of austenitic filler metals in paved tracks for the repair of the running surface defects of rails considering field tests. Facta Universitatis, Series: Mechanical Engineering, 2023, https://doi.org/10.22190/FUME230828032B

[19] A. Kuchak, D. Marinkovic, M. Zehn. Parametric investigation of a rail damper design based on a lab-scaled model. Journal of Vibration Engineering Technologies, Vol. 9, 2021, pp. 51-60, https://doi.org/10.1007/s42417-020-00209-2

[20] A. Kuchak, D. Marinkovic, M. Zehn. Finite element model updating–Case study of a rail damper. Structural Engineering and Mechanics, Vol. 73(1), 20220, pp. 27-35, http://doi.org/10.12989/sem.2020.73.1.027

[21] Y. Yan, J. Zhao, S. Ji, Discrete element analysis of breakage of irregularly shaped railway ballast. Geomechanics and Geoengineering, Vol. 10(1), 2014, pp. 1-9, https://doi.org/10.1080/17486025.2014.933891

[22] N. Kumar, B. Suhr, S. Marschnig, P. Dietmaier, C. Marte, K. Six. Micro-mechanical investigation of railway ballast behavior under cyclic loading in a box test using DEM: Effects of elastic layers and ballast types. Granular Matter, Vol. 21(4), 2019, 106, https://doi.org/10.1007/s10035-019-0956-9

[23] M. Esmaeili, R. Nouri, K. Yousefian. Experimental comparison of the lateral resistance of tracks with steel slag ballast and limestone ballast materials. Proceedings of the Institution of Mechanical Engineers Part F Journal of Rail and Rapid Transit, Vol. 231(2), 2016, pp. 175-184, https://doi.org/10.1177/0954409715623577

[24] Y. Guo, V. Markine, J. Song, G. Jing. Ballast degradation: Effect of particle size and shape using Los Angeles abrasion test and image analysis.

Construction and Building Materials, Vol. 169, 2018, pp. 414-424, https://doi.org/10.1016/j.conbuildmat.2018.02.170

[25] M. Esmaeili, M. Siahkouhi. Tire-derived aggregate layer performance in railway bridges as a novel impact absorber: Numerical and field study. Structural Control and Health Monitoring, Vol. 26(10), 2019, e2444, https://doi.org/10.1002/stc.2444

[26] Y. Alabbasi, M. Hussein. Large-scale triaxial and box testing on railroad ballast: A review. SN Applied Sciences, Vol. 1(12), 2019, 1592, https://doi.org/10.1007/s42452-019-1459-3

[27] B. Czinder, B. Vásárhelyi, Á. Török. Long-term abrasion of rocks assessed by micro-Deval tests and estimation of the abrasion process of rock types based on strength parameters. Engineering Geology, Vol. 282, 2021, 105996, https://doi.org/10.1016/j.enggeo.2021.105996

[28] E. Kuna, G. Bögöly. Overview of the Empirical Relations between Different Aggregate Degradation Values and Rock Strength Parameters. Periodica Polytechnica Civil Engineering, Vol. 68(2), 2024, pp. 375-391, https://doi.org/10.3311/PPci.22396

[29] F. Mengistu, H. Gebregziabher. Assessment of ballast flying in the national railway network of Ethiopia. Engineering, Vol. 13(7), 2021, pp. 420-429, https://doi.org/10.4236/eng.2021.137030

[30] Á. Orosz, Z. Farkas, Z., K. Tamás. Experimental investigation of mixing railway ballast grains with different form using large-scale direct shear box apparatus. Transportation Geotechnics, Vol. 42, 2023, 101105, https://doi.org/10.1016/j.trgeo.2023.101105

[31] E. Juhász, M. Movahedi Rad, I. Fekete, S. Fischer. Discrete element modelling of particle degardation of railway ballast material with PFC3d software. Nauka ta Progres Transportu, Vol. 2019(6), 2019, pp. 103-116, https://doi.org/10.15802/stp2019/194472

[32] J. Pierré, J. Passieux, J. Périé. Finite element stereo digital image correlation: framework and mechanical regularization. Experimental Mechanics, Vol. 57(3), 2016, pp. 443-456, https://doi.org/10.1007/s11340-016-0246-y

[33] B. Indraratna, N. Ngo, C. Rujikiatkamjorn. Performance of ballast influenced by deformation and degradation: laboratory testing and numerical modeling. International Journal of Geomechanics, Vol. 20(1), 2020, 04019138, https://doi.org/10.1061/(asce)gm.1943-5622.0001515

[34] G. Fernandes, E. Palmeira, & R. Gomes, "Performance of geosynthetic-reinforced alternative sub-ballast material in a railway track", Geosynthetics International, Vol. 15, No. 5, pp. 311-321, 2008, https://doi.org/10.1680/gein.2008.15.5.311

[35] F. Benedetto, F. Tosti, A. Alani. An entropy-based analysis of gpr data for the assessment of railway ballast conditions. IEEE Transactions on Geoscience and Remote Sensing, Vol. 55(7), 2017, pp. 3900-3908, https://doi.org/10.1109/tgrs.2017.2683507

[36] Internet law library (2024, April 16) https://eur-lex.europa.eu/legal-content/hu/TXT/?uri=CELEX:32011R0305

[37] Internet law library (2024, April 16) https://net.jogtar.hu/jogszabaly?docid=a1300275.kor

[38] European Committee for Standardization, 2003, MSZ EN 13450, Aggregates for railway ballast, 33 p.

[39] European Committee for Standardization, 2024, MSZ EN 1097-1, Tests for mechanical and physical properties of aggregates. Part 1: Determination of the resistance to wear (micro-Deval), 23 p.

[40] European Committee for Standardization, 2020, MSZ EN 1097-2, Tests for mechanical and physical properties of aggregates. Part 2: Methods for the determination of resistance to fragmentation, 44 p.

[41] E. Árpás, G. Emszt, M. Gálos, L. Kárpáti. The Los Angeles test in the European standardisation system. Epitoanyag - Journal of Silicate Based and Composite Materials, Vol. 54(4), 2002, pp. 106-111, https://doi.org/10.14382/epitoanyag-jsbcm.2002.18

[42] European Committee for Standardization, 2012, EN 13286-2/AC, Unbound and hydraulically bound mixtures. Part 2: Test methods for laboratory reference density and water content. Proctor compaction, 30 p.

[43] A. Mohajerani, B. T. Nguyen, Y. Tanriverdi, K. Chandrawanka. A new practical method for determining the LA abrasion value for aggregates. Soils and Foundations, Vol. 57(5), 2017, pp. 840-848, https://doi.org/10.1016/j.sandf.2017.08.013

[44] B. Indraratna, W. Salim, C. Rujikiatkamjorn. Advanced rail geotechnology – Ballasted track. CRC Press Taylor & Francis Group, London, 2011

[45] B. Lichtberger. Track compendium. Eurailpress Tetzlaff-Hestra GmbH & Co. KG, Hamburg, 2005